

## Electron dynamics and plasma jet formation in a helium atmospheric pressure dielectric barrier discharge jet

Q. Th. Algwari and D. O'Connell

Citation: [Applied Physics Letters](#) **99**, 121501 (2011); doi: 10.1063/1.3628455

View online: <http://dx.doi.org/10.1063/1.3628455>

View Table of Contents: <http://scitation.aip.org/content/aip/journal/apl/99/12?ver=pdfcov>

Published by the [AIP Publishing](#)

---

### Articles you may be interested in

[Helium atmospheric pressure plasma jets touching dielectric and metal surfaces](#)

J. Appl. Phys. **118**, 013301 (2015); 10.1063/1.4923345

[Simulation of helium discharge ignition and dynamics in thin tubes at atmospheric pressure](#)

Appl. Phys. Lett. **99**, 161504 (2011); 10.1063/1.3655199

[An atmospheric pressure quasiuniform planar plasma jet generated by using a dielectric barrier configuration](#)

Appl. Phys. Lett. **98**, 241501 (2011); 10.1063/1.3599845

[Atmospheric pressure plasma jets beyond ground electrode as charge overflow in a dielectric barrier discharge setup](#)

J. Appl. Phys. **108**, 033302 (2010); 10.1063/1.3466993

[Self-organized pattern formation of an atmospheric pressure plasma jet in a dielectric barrier discharge configuration](#)

Appl. Phys. Lett. **90**, 221504 (2007); 10.1063/1.2745204

---

The image shows the cover of the journal Applied Physics Reviews. It features a blue and orange color scheme with a molecular structure background. The text 'AIP Applied Physics Reviews' is at the top left. The main title 'NEW Special Topic Sections' is in large white letters. Below it, 'NOW ONLINE' is in orange, followed by 'Lithium Niobate Properties and Applications: Reviews of Emerging Trends' in white. The AIP logo and 'Applied Physics Reviews' are at the bottom right.

**NEW Special Topic Sections**

**NOW ONLINE**  
Lithium Niobate Properties and Applications:  
Reviews of Emerging Trends

**AIP** Applied Physics  
Reviews

# Electron dynamics and plasma jet formation in a helium atmospheric pressure dielectric barrier discharge jet

Q. Th. Algwari<sup>1,2,a)</sup> and D. O'Connell<sup>1,3</sup>

<sup>1</sup>*Centre for Plasma Physics, School of Maths and Physics, Queen's University Belfast, University Road, Belfast, Northern Ireland BT7 1NN, United Kingdom*

<sup>2</sup>*Electronic Department, College of Electronics Engineering, Mosul University, Mosul 41002, Iraq*

<sup>3</sup>*York Plasma Institute, Department of Physics, University of York, York YO10 5DD, United Kingdom*

(Received 30 March 2011; accepted 3 August 2011; published online 19 September 2011)

The excitation dynamics within the main plasma production region and the plasma jets of a kHz atmospheric pressure dielectric barrier discharge (DBD) jet operated in helium was investigated. Within the dielectric tube, the plasma ignites as a streamer-type discharge. Plasma jets are emitted from both the powered and grounded electrode end; their dynamics are compared and contrasted. Ignition of these jets are quite different; the jet emitted from the powered electrode is ignited with a slight time delay to plasma ignition inside the dielectric tube, while breakdown of the jet at the grounded electrode end is from charging of the dielectric and is therefore dependent on plasma production and transport within the dielectric tube. Present streamer theories can explain these dynamics. © 2011 American Institute of Physics. [doi:10.1063/1.3628455]

Non-thermal atmospheric pressure plasma jets are of particular technological interest. They have the capability of delivering a unique reactive dry chemistry at room temperature and pressure to delicate surfaces. With improved understanding of these devices, there is potential to control defined compositions of reactive species for surface modifications and bio-medical applications, such as in plasma medicine.<sup>1,2</sup> In this paper, we examine the electron dynamics to identify the plasma sustainment mechanisms within the main plasma production region and energy transport through the interface to the plasma jet.

Many different kinds of cold plasma jets have been developed with different electrode configurations, as well as power input, e.g., rf, kHz.<sup>3,4</sup> One such configuration is a dielectric barrier discharge (DBD) jet.<sup>5-7</sup> Dielectric insulators in front of the electrodes suppress arcs and thermal instabilities are suppressed due to plasma pulsing, relatively high gas flows, and use of carrier gasses with high heat conductivity such as helium. Relatively long plasma plumes offer the advantage of transporting relevant plasma species to substrates for application. The plasma jet T-tube configuration is motivated and designed such that the plasma jets and their origin at both the powered and grounded electrode side can be simultaneously investigated. A diagram of the experimental setup is shown in Figure 1(a). The plasma jet is generated inside a quartz tube of inner diameter 4 mm and outer diameter 6 mm. Two tubular electrodes surround the quartz tube forming a DBD-type configuration. A distance of 25 mm separates the electrodes. A high voltage pulse source (Haiden, PHK-2k) with a repetition rate of 20 kHz and voltage amplitude of 6 kV was applied across the electrodes for the investigations presented here. A high-voltage probe (Tektronix, P6015) and a calibrated Rogowski coil (Pearson) connected to a digital oscilloscope (LeCroy WavePro 7300A) were used to measure the time dependent applied voltage

and current. The voltage and current over one 20 kHz cycle is plotted in Figure 1(b).

Helium gas of 4 slm flows through the main arm of the tube so that it symmetrically enters the dielectric barrier discharge with 2 slm of gas owing through each end. Relatively long plasma plumes are emitted from the plasma source, at both the powered and electrode ends, and propagate into free space in the helium gas channel. These plumes, while continuous to the naked eye, are in fact transient and consist of a series of plasma pulses when imaged on a nanosecond time scale. The plasma pulses are often referred to as plasma bullets.<sup>8</sup> The plasma pulses have a velocity a lot greater than the gas flow velocity, and are sustained through a streamer-like mechanism.<sup>9</sup> It should be noted that the dynamics of the light emission both inside the discharge and within both plasma jets was also measured and compared to that in linear devices (not shown), where the gas flow enters at one end of the glass tube, and the principle characteristics discussed in the following do not differ.

The time resolved emission within the kHz cycle is measured on a nanosecond timescale providing non-invasive access to the plasma jet excitation dynamics. Optical emission from three regions of the plasma jet is imaged onto an ICCD camera (Andor DH 520): the main plasma production region between the two electrodes, the jet produced at the grounded electrode side, and the jet produced at the powered electrode side. Two-dimensional space and time resolved images of the optical emission in each of these three regions is measured using a gate width of 20 ns in 20 ns intervals. The emission is very reproducible and measured from a single cycle and not averaged over several cycles. This emission is measured both perpendicular and in the line of propagation of the plasma jets (i.e., electric field and gas flow direction). In the line of propagation of the plasma jet, the emission is collected, with a variable focal length using a telescope (Navtar 1-6010), synchronised to the phase corresponding to the perpendicular position of the head of the plasma pulse.

<sup>a)</sup>Electronic mail: qnajim03@qub.ac.uk.

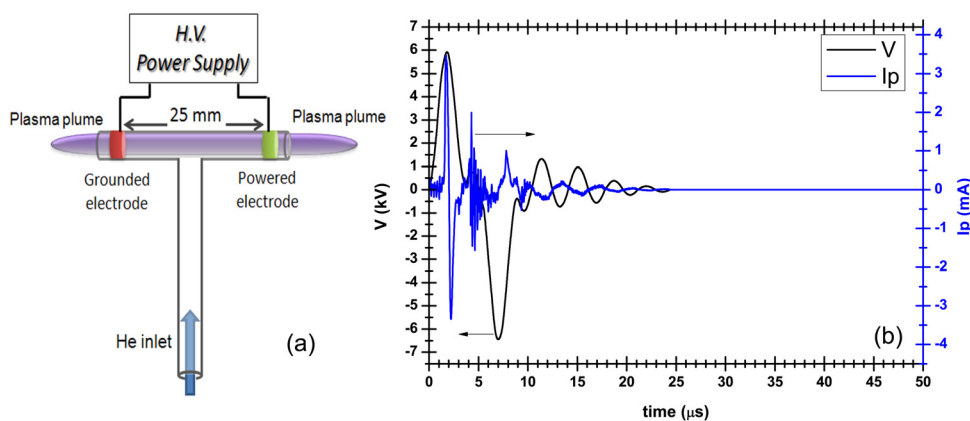


FIG. 1. (Color online) (a) Experimental DBD T-tube design operated in helium gas and (b) current and voltage waveform over one 20 kHz excitation cycle for applied voltage amplitude of 6 kV.

Optical emission is observed for duration of approximately  $2 \mu\text{s}$  during the positive half cycle of the voltage pulse. Figure 2 shows the axial spatial-temporally measured total emission during this phase between the two electrodes inside the quartz tube (22–48 mm), outside in the jet at the grounded electrode (0–17 mm), and the jet at the powered electrode (52–76 mm). From Figure 2, we can observe that plasma breakdown initiates close to the powered electrode inside the quartz tube (45 mm) at around  $0.8 \mu\text{s}$ , and with a slight time delay of less than  $0.3 \mu\text{s}$  breakdown occurs to the outside of the powered electrode close to ambient air near the end of the quartz tube. The later excitation is the jet observed at the powered electrode and will be discussed later in detail. The dynamics inside the tube can be observed in the movie attached to Figure 2. After breakdown inside the tube, the plasma initially propagates with a constant velocity of  $23.5 \text{ km}^{-1}$  towards the grounded electrode, and it then starts to accelerate and as it does so constricts until it reaches the grounded electrode. At the grounded electrode, the plasma dissipates onto the inner surface of the dielectric tube. While the ionisation wave itself propagates opposite to the electron drift, the magnitude of the ionisation wave velocity is comparable to the estimated electron drift velocity (assuming an electron mobil-

ity  $\mu_e$  of  $0.113 \text{ m}^2/\text{Vs}$  (Ref. 10)). All observations can be explained in the following picture. Breakdown starts in the form of an electron avalanche, where electrons are accelerated in the high electric field region of the externally applied electric field close to the powered electrode. As the density of the avalanche increases space charge effects become increasingly important significantly modifying the electric field. At this point, an avalanche to streamer transition occurs and the plasma will propagate under the collective influence of the external and self-generated electric field. The interior of the plasma streamer column consists of conducting plasma surrounded by a layer of space charge, so that the streamer interior electric field is largely screened. Space charges at the front of the plasma column create an electric field, causing electron multiplication, large enough to form an ionisation wave propagating as plasma pulses. Positive streamers propagate against the electron drift direction and thus need a source of free electrons ahead of the streamer in order to propagate; this source can be photo-ionization close to the streamer tip or background ionization. For our conditions, we can expect both secondary electron emission from the dielectric and previous discharge remnants to contribute to background ionisation. The plasma is operated in a regime where the gas takes over 180 cycles to traverse the entire gap between the electrodes in the quartz tube and as such can be considered stationary; therefore, pre-ionization from previous discharges will be relevant. Air impurities, in particular oxygen, will aid photo-ionisation and it has been shown that for streamer discharges even small levels of oxygen (1 ppm in pure nitrogen) are sufficient to enable this mechanism without the need for any background ionization.

Figure 2 also shows the plasma jet formation at both the powered and grounded electrodes. The origin of each of these jets and their propagation dynamics is considerably different and is discussed below in conjunction with Figures 3 and 4. Figure 3 and 4 show the distance travelled by the plasma pulses, as a function of time, for the jet created at the grounded electrode side and the powered electrode side, respectively. The radial structure of the plasma pulse, as obtained from the line of propagation images, at different phases is displayed as insets in the plots. The focal length of the optical system is varied for each phase such that the head of the plasma pulse is imaged onto the ICCD.

In Figure 3, it can be observed that the plasma pulse emerges from the grounded electrode side with an annular structure and propagates with a constant velocity of  $36.6 \text{ km}^{-1}$

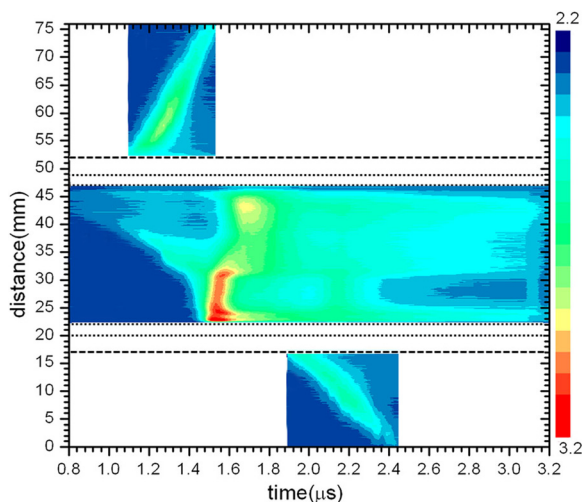


FIG. 2. (Color online) Spatio-temporal emission inside and outside the quartz discharge tube, between the electrodes (22 mm to 48 mm) and for each jet at the powered electrode (52 mm to 76 mm) and grounded electrode side (0 mm to 17 mm) for the same conditions as in Fig. 1. The attached movie shows the 2D spatio-temporal emission inside the two electrodes (powered electrode to the right and grounded electrode to the left) (enhanced online) [URL: <http://dx.doi.org/10.1063/1.3628455.1>].



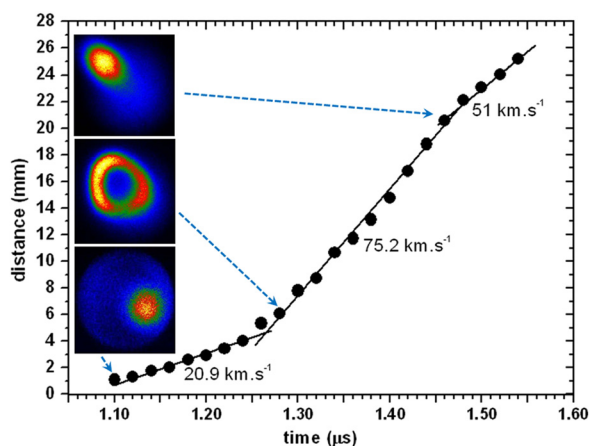


FIG. 3. (Color online) Distance of the head of the plasma pulse as a function of time for the plasma jet at the powered electrode side of the plasma tube for the same conditions as in Fig. 1. The insets represent the radial emission profile of the head of the plasma pulse at three different phases.

for approximately 15 mm before collapsing into a sphere and extinguishing. Upon emerging from the tube, the outside diameter of the plasma pulse annulus is equal to that of the inner diameter of the dielectric tube (4 mm). This jet is indirectly seeded from the plasma formed within the quartz tube. When the plasma ionization wave propagating inside the dielectric tube reaches the grounded electrode position, it dissipates onto the dielectric surface under the electrode (see movie of Figure 2). This initiates an ionisation wave, starting at  $1.5 \mu\text{s}$ , travelling along the inner surface of the tube, which in turn instigates the launch of an ionisation wave from the edge of the quartz tube (17 mm) into ambient air. Both charge dissipation and radiation impact on the dielectric surface are important for secondary breakdown. At  $1.5 \mu\text{s}$ , an ionization pulse is actually launched from the inner dielectric surface in two directions, to the outside resulting in the jet at the grounded electrode and a second back into the quartz tube. The excitation back into the plasma tube, while intense, only traverses about half the length of the tube before coming to rest and decaying over the next  $0.6 \mu\text{s}$ . As this excitation decays, another breakdown occurs ( $1.64 \mu\text{s}$ ) to the inside of the powered electrode, and this excitation does not propagate and is stagnant.

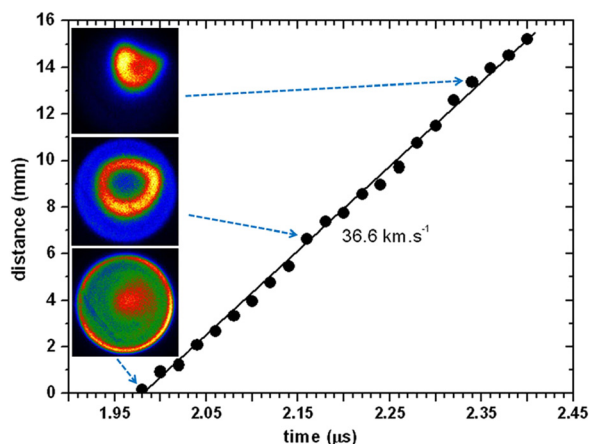


FIG. 4. (Color online) Distance of the head of the plasma pulse as a function of time for the plasma jet at the grounded electrode side of the plasma tube for the same conditions as in Fig. 1. The insets represent the radial emission profile of the head of the plasma pulse at three different phases.

In Figure 2 with a short time delay of  $0.3 \mu\text{s}$  to the initial plasma ignition inside the quartz tube at  $0.8 \mu\text{s}$ , another breakdown can be observed at the outer edge of the powered electrode (52 mm), and propagates away from the plasma tube into free space. This is the jet observed at the powered electrode. Earlier breakdown inside the tube compared with outside can be attributed to lower threshold breakdown voltage in the purer helium environment compared to that in ambient air with increased molecular densities. Although it should be noted that the density of oxygen and nitrogen impurities within the quartz tube is sufficient for efficient Penning ionization between helium metastables and molecular air impurities. The dynamics of the jet formed at the powered electrode is quite similar to the plasma propagation inside the tube; the jet is generated in the high electric field region of the externally powered electrode but then penetrates far beyond this into free space where the applied electric field can be expected to be below the plasma ionization threshold. Figure 4 shows the plasma pulse emitted from the powered electrode side initially ignites as a sphere structure propagating with a velocity of  $20.9 \text{ km s}^{-1}$ ; it then expands to an annular shape with an abrupt increase in velocity to  $75.2 \text{ km s}^{-1}$  and finally slows down again to  $51 \text{ km s}^{-1}$  as it collapses extinguishing as a sphere after 26 mm. The origin of the annular emission structure of the jet at the powered and grounded electrodes is very different. At the grounded electrode, the plasma pulse is seeded from the DBD inside the plasma tube, through the dielectric surface. On the other hand, the pulse at the powered electrode initiates as a sphere and acquires its annular structure downstream from ignition. This annulus can be attributed to mixing of ambient air with the helium gas channel, producing a maximum in radiation intensity off axis at a radial position where Penning ionisation, between helium metastables, in the plasma gas channel, and ambient air molecules, is most efficient. This annular structure arising from gas mixing has been observed by Sakiyama *et al.*, also in non-streamer rf driven atmospheric pressure plasma devices.<sup>11,12</sup>

The authors acknowledge support from UK EPSRC through a Career Acceleration Fellowship (EP/H003797/1) and one of the authors (Q.T.A.) acknowledges the support of the Iraqi Ministry of Higher Education and Scientific Research.

<sup>1</sup>D. O'Connell, L. J. Cox, W. B. Hyland, S. J. McMahon, S. Reuter, W. G. Graham, T. Gans, and F. J. Currell, *Appl. Phys. Lett.* **98**, 043701 (2011).

<sup>2</sup>J. Choi, K. Matsuo, H. Yoshida, T. Namiyama, S. Katsuki, and H. Akiyama, *Jpn. J. Appl. Phys.* **47**, 6459 (2008).

<sup>3</sup>K. Niemi, S. Reuter, L. M. Graham, J. Waskoenig, and T. Gans, *Appl. Phys. Lett.* **95**, 151504 (2009).

<sup>4</sup>K. Hyun, A. Brockhaus, and J. Engemann, *Appl. Phys. Lett.* **95**, 211501 (2009).

<sup>5</sup>J. L. Walsh and M. G. Kong, *Appl. Phys. Lett.* **89**, 231503 (2006).

<sup>6</sup>K. Urabe, T. Morita, K. Tachibana, B. Ganguly, *J. Phys. D: Appl. Phys.* **43**, 095201 (2010).

<sup>7</sup>W.-C. Zhu, Q. Li, X.-M. Zhu, and Y.-K. Pu, *J. Phys. D: Appl. Phys.* **42**, 202002 (2009).

<sup>8</sup>N. Mericam-Bourdet, M. Laroussi, A. Begum, and E. Karakas, *J. Phys. D: Appl. Phys.* **43**, 1209 (2010).

<sup>9</sup>L. Xinpei and M. Laroussi, *J. Appl. Phys.* **100**, 063302 (2006).

<sup>10</sup>Y. P. Raizer, *Gas Discharge Physics* (Springer, Berlin 1991).

<sup>11</sup>Y. Sakiyama and D. B. Graves, *Plasma Sources Sci. Technol.* **18**, 025022 (2009).

<sup>12</sup>Y. Sakiyama, N. Knake, D. Schroder, J. Winter, V. Schulz-von der Gathen, and D. B. Graves, *Appl. Phys. Lett.* **97**, 151501 (2010).